Journal of Alloys and Compounds 509 (2011) 3172–3176

Contents lists available at ScienceDirect

Journal of Alloys and Compounds

journal homepage: www.elsevier.com/locate/jallcom

Preparation and characterization of $La_{9.33}Si_6O_{26}$ powders by molten salt method for solid electrolyte application

Buyin Li, Jia Liu, Yunxiang Hu*, Zhaoxiang Huang

Department of Electronic Science & Technology, Huazhong University of Science & Technology, Wuhan, 430074, PR China

ARTICLE INFO

Article history:
Received 18 August 2010
Received in revised form 12 October 2010
Accepted 27 October 2010
Available online 13 December 2010

Keywords:
Lanthanum silicate
Molten salt method
Electrical conductivity
Powder synthesis

ABSTRACT

Lanthanum silicate $La_{9.33}Si_6O_{26}$ (LSO) powders with more uniform particle and less agglomeration were obtained at a much lower synthesis temperature by the molten salt method than by the solid-state method. LSO ceramic electrolytes were prepared with these powders and characterized as well. The optimal molten salt synthesis conditions are mass ratio of reactants to NaCl of 1:3 and synthesis temperature of 900 °C. XRD results showed that when the mass ratio of reactants to NaCl was no more than 1:3, pure LSO phase powder was obtained at 900 °C. XRD and XRF results showed that when synthesis temperature was higher than 900 °C, a solid solution type LSO powder with Na replacement for La formed at a fixed mass ratio of reactants to NaCl of 1:3. The involvement of Na in LSO lattice might lead to the lattice contraction in powders and deteriorate the conductance of ceramic electrolytes. The ceramic electrolytes prepared from the pure LSO powder via molten salt process exhibited better electrical properties than those from the powder via solid-state method.

1. Introduction

Solid oxide fuel cells (SOFCs) draw much attention in recent years, because of their high efficiency and environmentally friendly nature. A basic SOFC consists of three main ceramic components: an anode and a cathode separated by a solid electrolyte. Currently, yttria-stabilized zirconia (YSZ) with fluorite structure is the most common electrolyte material for SOFCs due to its excellent ionic conductivity and negligible electronic conduction at elevated temperatures (850–1000 °C), and good chemical stability. Nevertheless, this high operating temperature causes problems in terms of materials selection and lifetime [1–4]. So people search for alternative functional materials with higher ionic conductivity at relatively lower temperature [2,5]. The apatite structure materials as a new class of oxide-ion conductors for SOFCs, first found by Nakayama et al. [6,7], have high ionic conductivity at intermediate temperatures (700–800 °C), suitable thermal expansion matching with the electrode material, and other benefits [3–5,8]. The conduction mechanism of apatite structure materials is based on interstitial conduction and completely different from the oxygen vacancy conduction mechanism in the traditional materials with fluorite or perovskite related structures [5,9–11]. These apatite structure materials have a common chemical formula $Ln_{10-x}(MO_4)_6O_{2\pm y}$ (Ln is a metal such as rare earth or alkaline earth and M is a p-block element such as P, As, Si, or Ge), and $La_{9.33}SiO_6O_{26}$ (LSO) is a typical compound in this series [5,9,10,12–14]. Ln site ions can be partly replaced by other ion dopants with lower valance, and the conductivity of the resultant materials decreases with increasing dopant concentration if the ion radius of the dopants is smaller [15–20].

So far the preparation methods of LSO powders mainly include solid-state, sol–gel, and hydrothermal methods [9,12,13,21–24], while little study refers to the molten salt synthesis of them. In the molten salt process, the salt plays a role as flux. The reactants in the molten salt have a high reactivity and mobility, and react easily and completely, which can greatly reduce the synthesis temperature. Moreover the product powders have a better uniformity and fewer agglomerates [25]. These advantages are expected to be also embodied if molten salt method is applied to the synthesis of LSO powders.

The aim of the present paper is to explore the feasibility of the molten salt synthesis of LSO powders. The originality of this work is to decrease the synthesis temperature of LSO powders via the molten salt method and to obtain ultra-fine powders with narrow size distribution and dense ceramics with these powders. The effects of the mass ratio of reactants to the salt and the synthesis temperature on crystalline structure of the synthesized powders are investigated in detail.

2. Experimental procedures

Starting reactant powders of silicon dioxide (SiO_2, 98%) and lanthanum oxide (La_2O_3, 99%) were weighed in the nominal composition of $La_{9.33}Si_6O_{26}$. Sodium chloride (NaCl, 99%) was taken as the molten salt and weighed. The mass ratios of

* Corresponding author. Tel.: +86 27 87558482; fax: +86 27 87545167.
E-mail address: hyx@mail.hust.edu.cn (Y. Hu).

0925-8388/$ – see front matter © 2010 Elsevier B.V. All rights reserved.
doi:10.1016/j.jallcom.2010.10.215

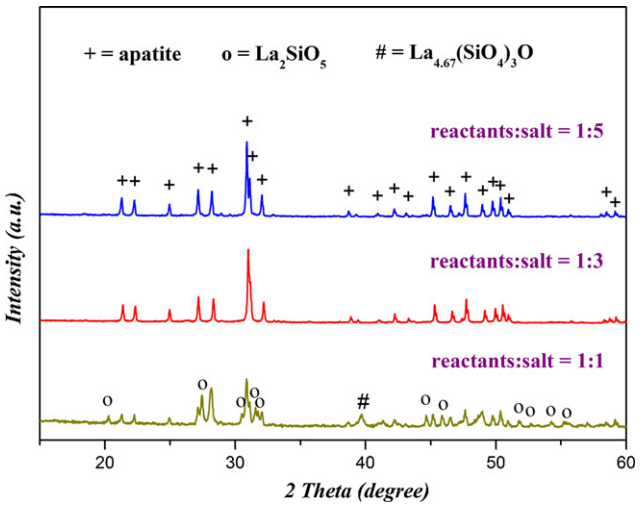

Fig. 1. XRD patterns of powders calcined at 900 °C for 4 h with different mass ratios of reactants to salt.

reactants to NaCl were fixed to be 1:1, 1:3, and 1:5 respectively. Then the mixtures of reactants and the salt were ball milled in ethanol medium for 4 h, dried, ground and sifted to avoid agglomerated powders. The sifted powders were calcined at 900–1100 °C for 4 h. Next, the as-synthesized powders were washed repeatedly with de-ionized water and filtered to remove free NaCl until there was no appearance of white precipitate in the filtrate by adding $AgNO_3$ solution. Finally LSO powders were obtained through drying the products at 105 °C for 6 h. In addition, for comparison a LSO powder was prepared by the solid-state reaction for 4 h at 1300 °C which is the lowest required temperature to synthesize the powder via traditional solid-state method.

The LSO powders were pelleted and pressed at 200 MPa for 25 s into disks (15 mm in diameter, 2 mm in thickness). The green disks were then heated to 1500 °C with a heating rate of 300 °C/h in air, soaked for 4 h, and then furnace-cooled.

X-ray diffraction (XRD) analyses at room temperature were carried out on a diffractometer (X'Pert PRO, PANalytical B.V.) using a Cu Kα radiation source ($K_{\alpha1}$ = 1.54060 Å and $K_{\alpha2}$ = 1.54443 Å). This method has been performed on each powder sample in order to reveal the crystallographic structures and cell parameters.

X-ray fluorescence (XRF) probe analyses (EAGLE III) were adopted to analyze qualitatively and semi-quantitatively the elemental composition of ceramic samples.

Scanning electron micrograph (SEM) analyses (Quanta 200, Philips) was used to observe the micromorphology of the synthesized powders and ceramics.

A. C. conductivity measurement of the ceramics was performed with an accurate impedance analyzer (Agilent 4294A) at frequencies of 40 Hz–20 MHz at temperatures of 300–800 °C.

3. Results and discussion

3.1. Synthesis and characterization of LSO powders

The effect of mass ratio of reactants to salt on the phase composition of synthesized powders was investigated. Fig. 1 shows the XRD patterns of powders calcined at 900 °C for 4 h with different mass ratios. It is apparent that no NaCl, La_2O_3, and SiO_2 peaks were detected in all synthesized powders, indicating that the presence of NaCl in the reactant mixture is helpful for the reaction between the reactants at relatively lower temperature (900 °C) and free NaCl can be completely removed from the product powders by washing repeatedly. Further, at lower salt concentration (reactants:salt = 1:1) apatite structure LSO phase (JCPDS 49-0443) formed with the companion of other impurity phases La_2SiO_5 (JCPDS 40-0234) and $La_{4.67}(SiO_4)_3O$ (JCPDS 75-1145). However, only did single LSO apatite phase exist at higher salt concentration (1:3 and 1:5). The XRD results indicate that there is a threshold salt concentration for the preparation of pure LSO powders which lies between 1:1 and 1:3. It seems that excess salt concentration (1:5) has no further help to the synthesis of pure LSO powders. Therefore the mass ratio of 1:3 was taken for the succeeding experiments.

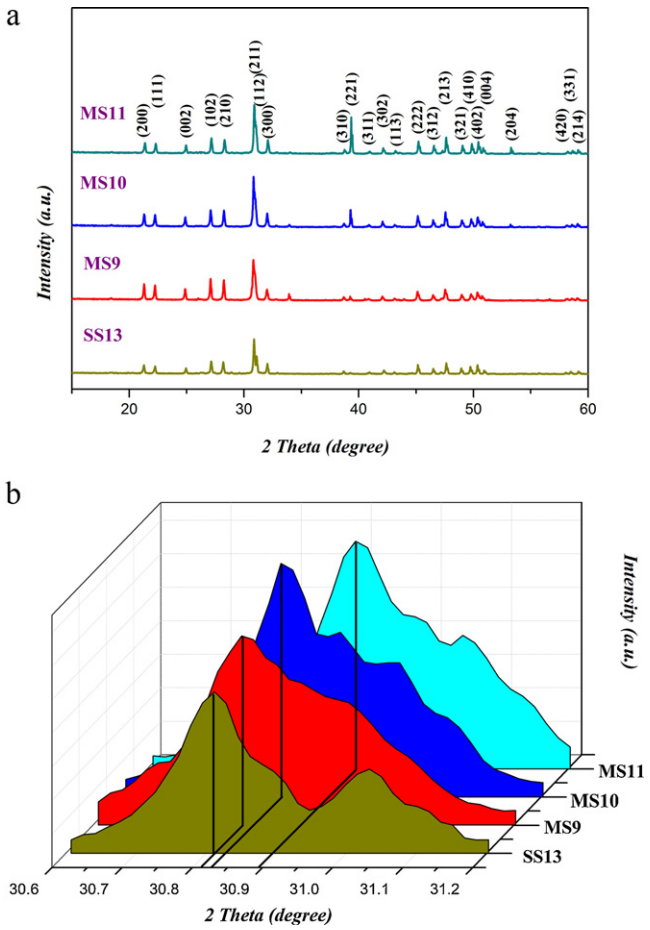

Fig. 2. (a) XRD patterns and (b) (2 1 1) peak magnification patterns of powders obtained at different synthesis temperatures by different methods.

In order to explore the effect of the synthesis temperature on the microstructure of LSO powders, powders were synthesized using molten salt method at 900, 1000, and 1100 °C for 4 h respectively with a fixed reactants to salt ratio of 1:3. For comparison, a powder was synthesized by the solid-state method at 1300 °C for 4 h. For simplification these four powders were named MS9, MS10, MS11, and SS13 respectively.

XRD patterns of these four powders are displayed in Fig. 2(a). They all had the same pure apatite structure characteristic peaks (JCPDS 49-0443), and no significant impure peaks appeared, indicating that pure apatite structure phase could be formed when reactant mixture was calcined at temperatures of 900–1100 °C for molten salt method while at 1300 °C for solid-state method. Moreover, it is apparent that MS9 had larger peak intensity than SS13 though MS9 was synthesized at a much lower temperature than SS13. This observation shows that the molten salt method allows the synthesis of LSO powders with better crystal growth at a relatively low temperature.

Furthermore, it is observed that the strongest (2 1 1) peak moved slightly to the right side in turn from MS9 to MS11 (Fig. 2(b)). According to Bragg's diffraction law, the (2 1 1) interplanar spacing in the synthesized powders decreased from MS9 to MS11. In order to prove this inference, the Philips X'pert Highscore software was used to calculate the cell parameters, and the results are shown in Table 1. For comparison parameters of SS13, and the standard LSO and $NaLa_9(SiO_4)_6O_2$ (JCPDS 32-1109) are also listed. It can be seen that cell parameters *a*, *b*, and *c* and cell volume *V* all decreased from MS9 to MS11. For SS13 and MS9 these parameters approached to those of

Table 1
Cell parameter comparison between the synthesized powders and standard LSO and $NaLa_9(SiO_4)_6O_2$.

	Standard LSO	SS13	MS9	MS10	MS11	Standard $NaLa_9(SiO_4)_6O_2$
Cell parameters *a*, *b* (Å)	9.7128	9.7108 ± 0.0032	9.7134 ± 0.0048	9.7022 ± 0.0028	9.6943 ± 0.0012	9.6920
Cell parameter *c* (Å)	7.1858	7.1906 ± 0.0041	7.1842 ± 0.0022	7.1824 ± 0.0015	7.1823 ± 0.0009	7.1820
Cell volume, *V* (Å^3)	587.08	587.22	587.02	585.51	584.56	584.26

Table 2
Conductance data, elemental composition, and average grain size for different ceramic samples.

	SS13	MS9	MS10	MS11
σ @ 800 °C (S/cm)	8.78×10^{-4}	1.09×10^{-3}	2.25×10^{-4}	1.58×10^{-4}
E_a (eV)	0.81	0.77	1.03	1.05
Na:La:Si (atom %)	0:57.83:42.17	0:56.23:43.77	6.52:47.68:45.8	13.83:49.01:37.16
Grain size (μm)	2.3	5.0	2.8	3.2

the standard LSO, while for MS11 to those of the standard $NaLa_9(SiO_4)_6O_2$.

The changes in (2 1 1) peak position and cell parameters from MS9 to MS11 might result from the involvement of Na ions in the reaction. Na^+ probably occupied in part the sites and the vacancy of La^{3+} and entered the LSO lattice at high temperatures, which led to the formation of a solid solution of $Na_xLa_{9.33-x/3}(SiO_4)_6O_2$. Since Na^+ has a slightly smaller radius (0.97 Å) than La^{3+} (1.06 Å), the replacement of Na^+ for La^{3+} led to decreased crystal parameters (i.e. lattice contraction). The presence of elemental Na in the synthesized powders via molten method was confirmed by the composition analysis on ceramics made from powders MS10 and MS11 through XRF (See Table 2). Notice that XRD results show absence of free NaCl in these powders. It can be concluded that Na existed in the form of solid solution in these powders. Furthermore no elemental Na was detected in SS13 and MS9 powders. Notice that the synthesis temperature increased from 900 °C for MS9 to 1100 °C for MS11. Therefore there was a synthesis temperature threshold for Na^+ replacing La^{3+} in the molten salt process, and when synthesis temperature exceeded this threshold the replacement amount increased with the increasing temperature.

Fig. 3 shows the SEM morphology of SS13 and MS9 powders. Both powders consisted of spherical shape particles. The mean particle size for MS9 was 250 ± 20 nm while 600 ± 100 nm for SS13. In addition MS9 had less agglomeration than SS13. The contrastive pictures directly confirm that molten salt method allows the synthesis of homogeneous LSO powders with smaller crystallites at a much lower temperature compared with solid-state method. These particles can be used to prepare dense ceramics.

3.2. Preparation and characterization of LSO ceramics

LSO ceramics were sintered at 1500 °C in air for 4 h using SS13, MS9, MS10, and MS11 powders respectively. The bulk densities of SS13, MS9, MS10, and MS11 ceramic samples were 4.91, 5.04, 4.93, and 4.89 g cm^{-3}, respectively. Fig. 4 shows the SEM images of the four obtained ceramic samples. It can be seen that all these samples were very dense and could satisfy the application in SOFCs [12]. Furthermore, the three ceramic samples from molten salt method powders had a bigger average grain size than the one from solid-state method powder under the same sintering condition. The average grain sizes of these four ceramics were 2.3 μm (SS13), 5.0 μm (MS9), 2.8 μm (MS10), and 3.2 μm (MS11). Finally, the grains of the SS13 ceramic only developed 3.5 times than its

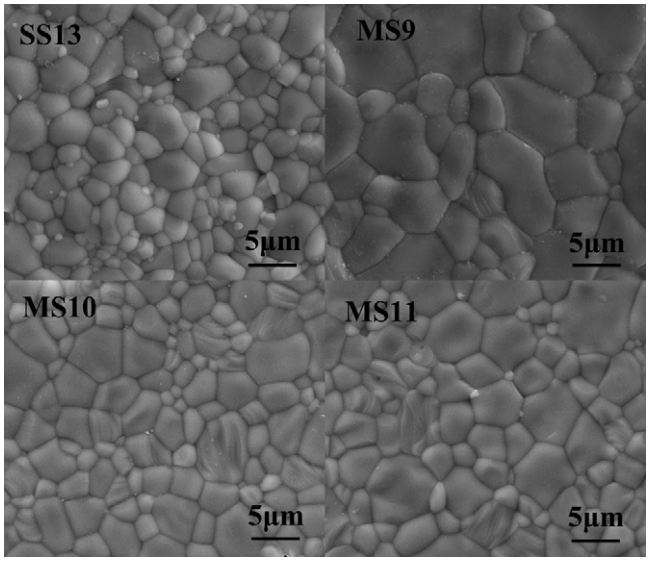

Fig. 4. SEM images of SS13, MS9, MS10, and MS11 ceramics sintered at 1500 °C in air for 4 h.

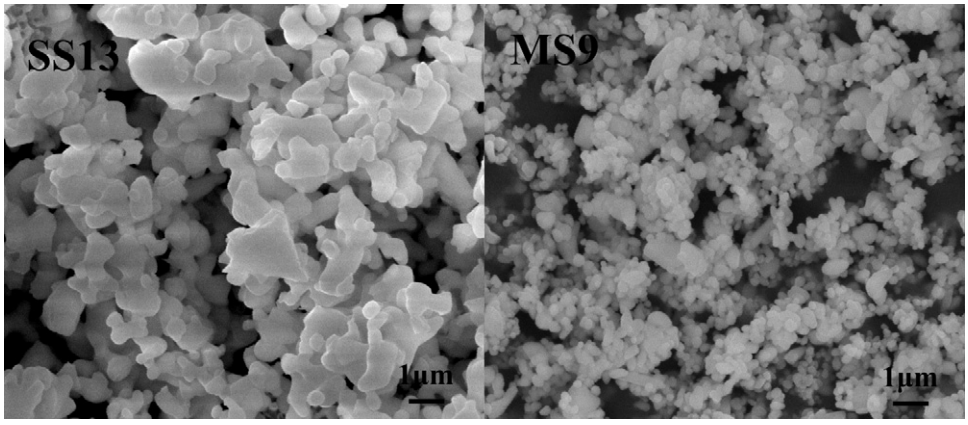

Fig. 3. SEM images of LSO powders prepared by solid-state method (SS13) and molten salt method (MS9).

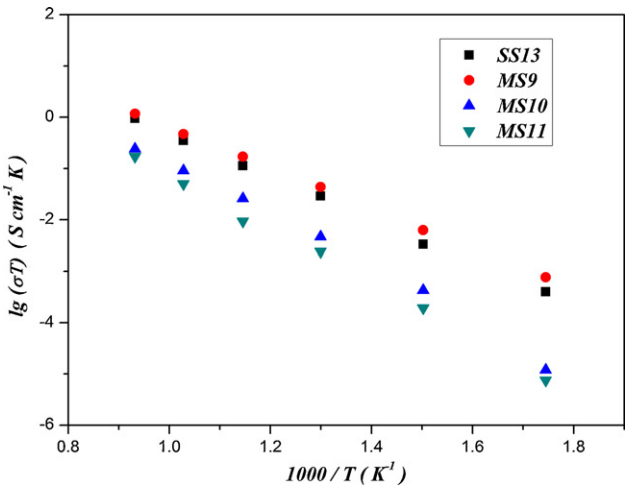

Fig. 5. Arrhenius plots of the overall electrical conductivity of LSO ceramics sintered from different powders.

staring powder (Fig. 3), while the growth multiple was about 20 times for the MS9 ceramic. This result indicated that the powders prepared by molten salt method had a higher growth activity than the powder by solid-state method.

The elemental composition results were listed in Table 2 for the four ceramic samples. The Na atomic ratio varied from zero in MS9 and SS13, 6.59% in MS10, to 13.83% in MS11. It is worth to stress that the Na atomic ratio increased from MS9, MS10, to MS11 ceramics, i.e. it increased with the increasing synthesis temperature of precursor powders by the molten salt method. This observation supports the conclusion that the replacement of Na^+ to La^{3+} took place in MS10 and MS11 powders while did not do in MS9 powder due to lower synthesis temperature.

In order to investigate the conductivity of these LSO ceramic electrolytes, silver paste as electrodes was applied to opposite faces of sintered pellets and then heated at 850 °C for 10 min for metallization. A. C. impedance measurement was performed on pellets at frequencies of 40 Hz–20 MHz at 300–800 °C. The obtained impedance spectrum showed substantial overlapping of the impedance arcs, and it is difficult to separate the grain bulk and grain boundary contribution from the impedance curve. Therefore, the total impedance is taken to calculate the conductivities of samples herein. These result data are parameterized by the Arrhenius equation:

$$\sigma = \frac{\sigma_0}{T} \exp\left(-\frac{E_a}{kT}\right) \quad (1)$$

where σ, σ_0, E_a, k, and T are, respectively, the conductivity, pre-exponential factor, activation energy, Boltzmann constant, and absolute temperature. Arrhenius plots of the four LSO ceramic samples are shown in Fig. 5.

First of all, for each ceramic sample, the conductivity increased when the temperature increased. Secondly, it can be seen that among the four samples the MS9 ceramics showed the most excellent conductance in the range of 300–800 °C, including the highest conductivity at every fixed temperature point and the lowest activation energy E_a (Table 2). The SS13 ceramics took the second best place while MS10 and MS11 ceramics exhibited the worst conductance. Finally, the conductivity discrepancy among samples became smaller with the increasing temperature. These phenomena will be explained in details as follows.

From MS9, MS10, to MS11 ceramic, the conductance became worse and worse, although their precursor powders all were prepared by the same way—molten salt method. This might originate from the differences in the average grain size and the amount of Na element in the ceramic samples. The density factor which was often considered elsewhere may be neglected here because all ceramic samples in this work were dense. As we know, the sum of grain bulk and grain boundary contributions was considered to determine the conductivity values for apatite materials [12]. MS9 had larger grains and therefore less grain boundaries in unit volume than MS10 and MS11 (Fig. 4), which led to MS9 having a better conductance than other two.

What is more important is that from MS9, MS10, to MS11 ceramic, the amount of Na element increased, and the involvement of Na deteriorated the conductance of electrolytes. It is well known that oxygen ions in the apatite silicates are confirmed to migrate via an interstitial conduction mechanism: excess oxide ions can be introduced in the structure and facilitate oxide-ion migration in the conduction channel by a complex sinusoidal pathway along the *c*-axis. Moreover, the pathway is strongly dependent on the ability of the silicate substructure to relax towards the La sites that contain the cation vacancies in the apatite structure [5,9–11]. The involvement of Na in LSO lattice could change the micro-conduction mechanism of samples by two ways. Firstly, the lattice contraction (see Table 1) and conduction channel narrowing caused by the incorporation of Na^+ ions might limit the oxide ions diffusion. Secondly, to maintain total charge balance in the composition, the replacement of lower valence ion Na^+ for La^{3+} certainly resulted in the reduction in the number of cation vacancies, which had a directly harmful influence on oxide ions migration to the interstitial site [15].

The reason for MS9 ceramic exhibited a better conductance than SS13 ceramic may be explained as follows. Notice that there was no Na element in both MS9 and SS13 ceramics. Furthermore, MS9 had a larger average grain size and therefore less grain boundaries than SS13 ceramic, which led to MS9 having a higher conductivity. However, although MS10 and MS11 ceramics had a slightly bigger grain size than SS13 ceramic, a much worse conductivity was observed for the former. This might be due to the adverse effects of Na in MS10 and MS11 on their conductance.

4. Conclusions

In summary, LSO powders with pure apatite phase were successfully synthesized at relatively low temperature via molten salt method. The optimal synthesis conditions are mass ratio of reactants to NaCl of 1:3 and synthesis temperature of 900 °C. When the mass ratio of reactants to NaCl was greater than 1:3, impurity phases existed in the powder synthesized at 900 °C. When synthesis temperature was higher than 900 °C, a solid solution type LSO powder with Na replacement for La formed at a fixed mass ratio of reactants to NaCl of 1:3. The involvement of Na in LSO lattice may be responsible for the lattice contraction in MS10 and MS11 powders and for the conductance deterioration in MS10 and MS11 ceramic electrolytes. Ceramic electrolytes prepared from the pure LSO molten salt powder (MS9) exhibited better electrical properties than those from the solid-state powder (SS13).

References

[1] G.J. Offer, J. Mermelstein, E. Brightman, N.P. Brandon, J. Am. Ceram. Soc. 92 (2009) 763–780.
[2] A. Orera, P.R. Slater, Chem. Mater. 22 (2010) 675–690.
[3] K. Huang, J. Wan, J.B. Goodenough, J. Mater. Sci. 36 (2001) 1093–1098.
[4] Y. Higuchi, M. Sugawara, K. Onishi, M. Sakamoto, S. Nakayama, Ceram. Int. 36 (2010) 955–959.
[5] T. Kharlamova, S. Pavlova, V. Sadykov, T. Krieger, L. Batuev, V. Muzykantov, N. Uvarov, C. Argirusis, Solid State Ionics 180 (2009) 796–799.
[6] S. Nakayama, H. Aono, Y. Sadaoka, Chem. Lett. 6 (1995) 431–432.
[7] S. Nakayama, M. Sakamoto, J. Eur. Ceram. Soc. 18 (1998) 1413–1418.
[8] D. Marrero-López, M.C. Martín-Sedeno, J. Pena-Martínez, J.C. Ruiz-Morales, P. Núnez, M.A.G. Aranda, J.R. Ramos-Barrado, J. Power Sources 195 (2010) 2496–2506.

[9] L. León-Reina, J.M. Porras-Vázquez, E.R. Losilla, M.A.G. Aranda, Solid State Ionics 177 (2006) 1307–1315.
[10] T. Iwata, E. Bechade, K. Fukuda, O. Masson, I. Julien, E. Champion, P. Thomas, J. Am. Ceram. Soc. 91 (2008) 3714–3720.
[11] L. Leon-Reina, E.R. Losilla, M. Martınez-Lara, S. Bruque, A. Llobet, D.V. Sheptyakovc, M.A.G. Aranda, J. Mater. Chem. 15 (2005) 2489–2498.
[12] P.J. Panteix, I. Julien, D. Bernache-Assollant, P. Abelard, Mater. Chem. Phys. 95 (2006) 313–320.
[13] T. Nakajima, K. Nishio, T. Ishigaki, T. Tsuchiya, J. Sol–Gel Sci. Technol. 33 (2005) 107–111.
[14] P.J. Panteix, I. Julien, P. Abelard, D. Bernache-Assollant, Ceram. Int. 34 (2008) 1579–1586.
[15] P.J. Panteix, E. Bechade, I. Julien, P. Abelard, D. Bernache-Assollant, Mater. Res. Bull. 43 (2008) 1223–1231.
[16] P.J. Panteix, I. Julien, P. Abelard, D. Bernache-Assollant, J. Eur. Ceram. Soc. 28 (2008) 821–828.
[17] E. Kendrick, K.S. Knight, P.R. Slater, Mater. Res. Bull. 44 (2009) 1806–1809.
[18] E. Kendrick, P.R. Slater, Solid State Ionics 179 (2008) 981–984.
[19] E. Kendrick, A. Orerac, P.R. Slater, J. Mater. Chem. 19 (2009) 7955–7958.
[20] J.R. Tolchard, P.R. Slater, M.S. Islam, Adv. Funct. Mater. 17 (2007) 2564–2571.
[21] S. Kato, T. Yoshizawa, N. Kakuta, S. Akiyama, M. Ogasawara, T. Wakabayashi, Y. Nakahara, S. Nakata, Res. Chem. Intermed. 34 (2008) 703–708.
[22] A. Chesnaud, G. Dezanneau, C. Estournès, C. Bogicevic, F. Karolak, S. Geiger, G. Geneste, Solid State Ionics 179 (2008) 1929–1939.
[23] S. Zec, J. Dukic, M. Puševac, S. Boškovic, R. Petrovic, Mater. Manuf. Process. 24 (2009) 1104–1108.
[24] S.H. Jo, P. Muralidharan, D.K. Kim, Electrochim. Acta 54 (2009) 7495–7501.
[25] P. Afanasiev, C. Geantet, Coord, Chem. Rev. 178 (1998) 1725–1752.